Asian Journal of Information Technology 5 (12): 1394-1409, 2006

Experimental and Theoretical Study of the Effects of Operating Parameters on Nitric Oxide Emissions from Spark-Ignition Engines

[1]Tayeb Ouksel, [2]Mahfoud Kadja, [3]Pascal Higelin and Abdelaziz Chelghoum
[1]Institute of Mechanics, University Center of Oum El Bouaghi, Algeria
[2]Laboratory of Appliqued Energetics and Pollution,
Département of Mechanics, University of Constantine, Algeria
[3]Laboratory of Mechanics and Energetics of the Polytechnic School,
University of Orleans, France

Abstract: The article reports the experimental and theoretical results for an engine working with petrol 95 as a fuel. The theoretical part of this work uses a multi-zone model in order to predict engine performance and NO emissions in a spark-ignition engine. The gas exchange process is calculated by one dimensional isentropic flow through a nozzle. During combustion, 11 products are obtained by chemical equilibrium and Nitric Oxide (NO) formation is calculated by the extended Zeldovich mechanism. The results of the computer multi-zone model are compared with the experimental data. The calculated values for pressure and NO emissions show good agreement with the experimental data. The multizone formulation developed here indicates that the use of 10 burned zones are likely to be sufficient for the accurate prediction of NO emission from SI engines.

Key words: Combustion, spark-ignition engines, nox, multizone model, dissociation

INTRODUCTION

The exhaust emissions from Internal Combustion Engines account for a major portion of the urbain air pollution. The three main pollutants which are subject to exhaust emission legislation are Carbon Monoxide (CO), unburned Hydrocarbons (HC) and Nitrogen Oxides (NO).

Nitric oxide which exhausts from the engine reacts with Hydrocarbons (HC) in sunlight to form ozone and photochemical smog. The NO can increase the frequency of respiratory diseases and contribute to the phenomenon of acid rains, which have harmful effects on the plants.

Knowledge and understanding of the effect of engine design and operating parameters on nitric oxide emissions from SI engines continues to be of utmost importance. Although this topic has been extensively studied since at least the late 1950s, both experimental and computational work continues on this important subject. Reaction kinetics are extremely sensitive to temperature variations so that an accurate description of the combustion chamber temperature field is a prerequisite for reliable NO predictions.

Patterson and van Wylen[1] reported one of the first thermodynamic simulations that included unburned and burned zones, progressive combustion, heat transfer and flame propagation for homogeneous charge engines. Their simulation did not, however include flow rates and heat transfer from the unburned zone. This simulation was the start of a long history of the development and use of thermodynamic engine simulations.

Krieger and Borman[2] reported the development of a two-zone engine cycle simulation. This work extended the capabilities of cycle simulation to include more detailed description of the fluid properties and the combustion process. Cycle simulation were presented for both spark-ignition and compression-ignition engines.

Lavoie *et al.*[3] took the measured pressure-crank angle data from the engine, in order to determine the temperature-crank angle history of unburned and burned gas elements. The thermodynamic model assumes constant specific heats for both burned and unburned gases so that analytical expressions can be obtained for the mean temperature of both gases. The authors assume no heat transfer from the system and consider two limiting cases for the burned gas:

- Uniform temperature and composition of the gases, corresponding to a « fully mixed » or two-zone model
- No mixing of burned gases, with each element isentropically compressed after combustion based on a value of gamma for the burned gases chosen to match equilibrium data over a range of temperature. The NO rate equations are integrated for each element from combustion to the end of expansion.

Corresponding Author: Tayeb Ouksel, Institute of Mechanics, University Center of Oum El Bouaghi, Algeria

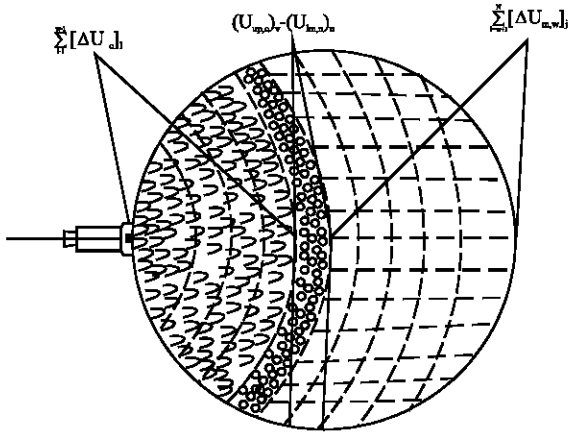

Fig. 1: Decomposition of the combustion chamber in many zones

Blumberg and Kummer[4] extended the model of Lavoie *et al.*[3] to include a mass fraction burned profile and the effect of fuel type, spark timing, fuel-air ratio and humidity.The model still incorporates the approximation of constant specific heat for the burned gas.

Heywood *et al.*[5] and Blumberg *et al.*[6] reported a description of examples of simulations using multiple zone for the combustion process in conjunction with computing nitric oxide emissions. For these simulations, the burned zone was divided into an adiabatic core and a boundary layer zone in addition to the unburned zone.

Lavoie and Blumberg[7] used multiple zone for the combustion process in conjunction with computing nitric oxide emissions. They noted that the use of a boundary layer zone allows a better representation of the heat loss which is known to be confined largely to the region near the walls.

James[8] also concluded that a multizone formulation was needed for the accurate prediction of NO, in order to take proper account of the temperature gradient in the burned gas.

Recent work on nitric oxide emissions from engines has been reported, for example by Miller *et al.*[9], Rublewski and Heywood[10], Stone *et al.*[11] and Caton[12-15].

The present paper discusses the experimental and theoretical results on nitric oxide emissions from spark-ignition engines. In order to obtain the theoretical results, the combustion process has been divided into 10 periods of equal burned mass fraction Fig. 1. The experimental data was obtained using a single cylinder, four stroke engine.

MATERIALS AND METHODS

Chemistry of combustion: In each burning zone, the eleven species CO_2, CO. H_2O H_2, OH O_2 O NO, N_2 H and N were computed. The combustion products are defined by dissociation considerations. The following equations were used:

$$\frac{1}{2}.H_2 \overset{(1)}{\leftrightarrow} H;\quad \frac{1}{2}.O_2 \overset{(2)}{\leftrightarrow} O;\quad \frac{1}{2}.N_2 \overset{(3)}{\leftrightarrow} N;\quad \frac{1}{2}.H_2 + \frac{1}{2}.O_2 \overset{(4)}{\leftrightarrow} OH$$

$$\frac{1}{2}.N_2 + \frac{1}{2}.O_2 \overset{(5)}{\leftrightarrow} NO;\quad H_2 + \frac{1}{2}.O_2 \overset{(6)}{\leftrightarrow} H_2O;$$

$$CO + \frac{1}{2}.O_2 \overset{(7)}{\leftrightarrow} CO_2$$

For a precise zone of combustion, where local gas temperature, pressure, excess air ratio and residual gas molar fraction are given, the concentration of each one of the above species can be calculated by solving a system of 11 equations, consisting of 4 from balance equations (one for each element C-H-O-N) and 7 equilibrium equations.

The calculation was based on the equilibrium assumption, except for NO formation for which the following model was used.

Nitric oxide formation model: The major source of nitric oxide is oxidation of nitrogen in the combustion air (Thermal NO).The Zel'dovich mechanism for thermal NO is well established:

$$N_2 + O \underset{k_{r1}}{\overset{k_{d1}}{\Leftrightarrow}} N + NO$$

$$O_2 + N \underset{k_{r2}}{\overset{k_{d2}}{\Leftrightarrow}} O + NO$$

In addition, the reaction between nitrogen and the hydroxyl radicals (OH) may be important for rich flames:

$$N + OH \underset{k_{r3}}{\overset{k_{d3}}{\Leftrightarrow}} NO + H$$

The reaction below also contributes to the formation of NO in lean mixtures:

$$N_2 + O_2 \underset{k_{r4}}{\overset{k_{d4}}{\Leftrightarrow}} NO + NO$$

Two assumptions are used:

- The content of N is small and changes slowly compared to the content of NO.
- Concentration of O, O_2, OH, H and N_2 can be approximated by their equilibrium concentrations.

With these assumptions the following expression for NO formation is described:

$$\frac{d[NO]}{dt} = 2.\left(1-\beta^2\right).\left\{\frac{R_{1e}}{\beta.\frac{R_{1e}}{R_{2e}+R_{3e}}+1}+R_{4e}\right\} \quad (1)$$

Where

$$R_{1e} = k_{d1}.\left[N_2\right]_e.[O]_e = k_{r1}.[N]_e.[NO]_e$$

$$R_{2e} = k_{d2}.\left[O_2\right]_e.[N]_e = k_{r2}.[O]_e.[NO]_e$$

$$R_{3e} = k_{d3}.[N]_e.[OH]_e = k_{r3}.[H]_e.[NO]_e$$

$$R_{4e} = k_{d4}.\left[N_2\right]_e.\left[O_2\right]_e = k_{r4}.[NO]_e.[NO]_e$$

$$\beta = \frac{[NO]}{[NO]_e}$$

The concentration [ ] is in the unit (mol cm^{-3}) and the reaction rate constants are listed in tables given by Heywood[5]. The concentration [NO] is defined as:

$$[NO] = \frac{n_{NO}}{V}$$

Where n_{NO} is the quantity of NO in (mol) distributed in the volume V. For a constant volume V Eq. (1) can equivalently be written as:

$$\frac{1}{V}.\frac{d[NO]}{dt} = 2.\left(1-\beta^2\right).\left\{\frac{R_{1e}}{\beta.\frac{R_{1e}}{R_{2e}+R_{3e}}+1}+R_{4e}\right\}$$

For the purpose of calculating NO in internal combustion engines the following extension of Eq. 1 is proposed that accounts for a change in burned zone volume, V_b:

$$\frac{d[NO]}{dt} = 2.\left(1-\beta^2\right).\left\{\frac{R_{1e}}{\beta.\frac{R_{1e}}{R_{2e}+R_{3e}}+1}+R_{4e}\right\} - \frac{[NO]}{V_b}.\frac{dV_b}{dt} \quad (2)$$

An increase of cylinder volume will increase the burned zone volume and the concentration of NO in the burned zone decreases. The differential Eq. (2), which governs the variation of the concentration of nitric oxide resulting from combustion in zone ω as a function of crank-angle, is solved by the Runge-kutta method with a step of calculation equal to 1°.

The nitric oxide kinetics are integrated along the state-time histories and weighted and summed according to the mass-fraction burned model when the NO levels have frozen.

$$[NO] = \sum_{j=1}^{N_z}[NO]_j.\Delta X_j$$

Where N_z is the number of zones.

Heat release rate: The heat addition for spark ignition engines may be prescribed as a function of crank angle

For example, it is found that the following equation works reasonably well:

$$x(\varphi) = \frac{\left[1-\cos\left\{\frac{\pi.(\varphi-\varphi_0)}{\varphi_z}\right\}\right]}{2}$$

Where x(φ) is the fraction of the heat release, φ refers to crank angle, φ_0 is the start of heat release and φ_z is the duration of heat release. The above equation is applied only during the time of heat release. $\varphi_0 < \varphi < \varphi_0 + \varphi_z$.

A functional form often used to represent the mass fraction burned versus crank angle curve is the Wiebe function:

$$x(\varphi) = 1-\exp\left[-6.908.\left(\frac{\varphi}{\varphi_z}\right)^{m+1}\right]$$

Heat transfer to or from the charge: The instantaneous heat interaction between the cylinder content and its walls were calculated using the relationship:

$$\frac{dQ_{ht}}{dt} = h_c.A(\theta).\left(T-T_w\right)$$

Where h_c is the convective heat transfer coefficient, $A(\theta)$ is the total heat transfer surface area of the mixture, (m^2), T, the instantaneous mean charge temperature and T_w is the cylinder wall temperature.

In this work, the Woschni[16] formula was used for the calculation of the instantaneous convective heat transfer coefficient h_c.

$$h_c = 0.8195.P^{0.8}.W_c^{0.8}.D^{-0.2}.T^{-0.53}$$

Table 1: Coefficients C_1 and C_2 in the correlation of Woschni[16].

Phase of engine cycle	Coefficient C_1	Coefficient C_2
Gas exchange process	6,18	0
Compression	2,28	0
Combustion and expansion	2,28	$3,24.10^{-3}$

Where: P is the mean cylinder pressure, (MPa); W_c, the average gas velocity in the cylinder, (m/s); D, the bore, (m); T, is the varying mean charge temperature (K).

The characteristic gas velocity in the Woschni correlation W_c is proportional to the mean piston speed during intake, compression and exhaust. During combustion and expansion, it is assumed that the gas velocities are increased by the pressure rise resulting from combustion, so the characteristic gas velocity has both piston speed and cylinder pressure rise terms.

The average gas velocity in the cylinder W_c, is calculated using:

$$W_c = \left[C_1 . W_{mp} + C_2 . \frac{V_c . T_{EVC}}{P_{EVC} . V_{EVC}} . \left(P - P_{sa} \right) \right]$$

Where W_{mp} is the mean velocity of the piston,(m/s).

V_c is the cylinder clearance volume

Prediction of temperature field in the combustion chamber: The mass of gases at the beginning of the process of combustion is divided into 10 equal slices in mass, which burn successively one after the other in the increasing order of their numbering[1-4]. At every moment, one distinguishes the slices 1 to w-1 which consist of combustion products and the slices w+1 to 10 which consist of working mixture (air+fuel+residual gazes). The slice W is in the course of combustion.

The temperature of the burnt gases at the end of combustion in zone W is given by the equation expressing the first principle of thermodynamics

$$\Delta Q_w = \left(U''_{p.c} \right)_w - \left(U'_{m.m} \right)_w + \sum_{j=1}^{w-1} \left(\Delta U_{p.c} \right)_j + \sum_{j=w+1}^{N} \left(\Delta U_{m.m} \right)_j - \Delta L_w \quad (3)$$

Where ΔQ_w and ΔL_w are the released heat and work in zone w, $(U''_{p.c})_w$ is the internal energy of combustion products in zone w, $(U'_{m.m})_w$ is the internal energy of the initial mixture in zone w, $\sum_{j=1}^{w-1} \left(\Delta U_{p.c} \right)_j$ is the sum of variations of internal energy of the combustion products in the already burnt zones and $\sum_{j=w+1}^{N} \left(\Delta U_{m.m} \right)_j$ is the sum of variations of internal energy of the initial mixture in the yet unburnt zones.

Step-by-step numerical solution procedure

Computation of compression phase

3.1 .1 Introduce the data at IVC, i.e α_1, P_1, T_1 trapped composition and compute V_1 from engine geometry. From the perfect gas state equation calculate the trapped kmol of carbureted mixture n_{mc} and then the kmol of working-fluid $n_{mc}.(1+\gamma_r)$. Select crank angle step size $\Delta\alpha$ equal, here to 1°. Where γ_r is the residual fraction.

3.1 .2 For new crank angle $\alpha_2 = \alpha_1 + \Delta\alpha$, compute V_2 from engine geometry and then calculate the new temperature at the end of step from the following equation: $T_2 = T_1 + \Delta T$, where ΔT is the proposed increment of temperature in this step.

3.1 .3 Compute the mean temperature in this step $T_{1-2} = (T_1 + T_2)/2$, the mean isentropic exponent $\gamma_{1-2}\left(T_{1-2}\right) = 1.438 - \frac{1.05.T_{1-2}}{10^4}$ and the mean molar heat capacity $C_v\left(T_{1-2}\right) = \frac{R}{M_{mix} \cdot \left(\gamma_{1-2}\left(T_{1-2}\right) - 1 \right)}$.

3.1 .4 Find pressure P_2 at the end of step by integration of the first law of thermodynamics for a closed system $dU = \delta Q_h + \delta W$, where δQ_h is calculated from the heat loss sub-model of Woschni [16]:

$$\delta Q_h = h_c . \left(T - T_w \right) . S_w . \frac{d\alpha}{6.n}$$

$h_c = 3.26.B^{-0.2}.P^{0.8}.T^{-0.55}.w^{0.8}\ (W/m^2.K)$, is the convective heat transfer coefficient calculated from Woschni correlation[16].

Where:

B is the cylinder bore (m), P is the instantaneous cylinder pressure (KPa), T is the temperature (K) and w is the average cylinder gas velocity (m/s) determined from the following equation :

$$w = \left[C_1 . w_{mp} + C_2 . \frac{V_d . T_r}{P_r . V_r} . \left(P - P_m \right) \right]$$

where V_d is the displaced volume, P is the instantaneous cylinder pressure, P_r, V_r, T_r, are the working-fluid pressure, volume and temperature at some reference state (say IVC) and P_m is the motored cylinder pressure at the same crank angle as P, n is the rotational speed of the crankshaft (rev/min).

For the compression period: $C_1 = 2.28$ and $C_2 = 0$

For the combustion and expansion period: $C_1 = 2.28$ and $C_2 = 3.24.10^{-3}$

w_{mp} is the mean piston speed (m/s),

$T_w = \frac{\left(T_p.S_p + T_{cyl}.S_{cyl} + T_{cul}.S_{cul}\right)}{S_w(\alpha)}$ is the mean temperature of the walls (K)

$S_w(\alpha) = S_p + S_{cyl}(\alpha) + S_{cu}$ is the combustion chamber surface area (m^2), which varies with crank angle α, consists of the piston top, the cylinder walls and the bottom of the cylinder head.

3.1.5 Estimate temperature T_{2e} at the end of step by the following equation: $T_{2e} = T_1.\frac{P_2}{P_1}.\frac{V_2}{V_1}$

3.1.6 Repeat steps 3.1.3-3.1.5 until the error (T_{2e}-T_2) is negligible.

3.1.7 Calculate the work in the step $\delta W = \frac{\left(P_1 + P_2\right)\left(V_2 - V_1\right)}{2}$

3.1.8 Set conditions at the end of time step (index 2) as initial conditions for the next time step (new state, index 1) and repeat all steps from 3.1.2 to 3.1.7.

In order to accelerate the convergence of the numerical procedure, the increase in temperature ΔT for the next step is calculated by an extrapolation method ($\Delta T = T_{2e}$-T_2). One carries on using this method until α_2 equals the value at the start of spark timing (θ).

In the compression stroke, the cylinder contents are a mixture of fuel , air and residual gases from the previous cycle that had stayed in the clearance volume, i.e. fuel, O_2, N_2 and residual gases.

Computation of combustion phase:

3.2.1 Set conditions at the end of previous time step (old state, index 2) as initial conditions for the current time step (new state, index 1).

3.2.2 At the end of compression (start of combustion), one can calculate the amounts of the products CO, CO_2, H_2, H_2O, O_2 and N_2 according to the richness or the poorness of the carburated mixture. At higher temperature, dissociation reactions start and then other products start arising like O, N, NO, H and OH.

3.2.3 The model of simulation used is multizonal, i .e. breaks up the mass contained in the cylinder at the ignition time into 10 (ten) equal sections in burned mass fraction, which burn successively one after the other in the increasing order of their classification. At every moment, one distinguishes the slices from 1 to w-1 which consist of combustion products and the sections from w+1 to 10 which consist of working-fluid (air + fuel + residual gases). The section w is in the course of combustion Fig. 1.

3.2.4 Dissociation reactions are generally endothermic, one characterises in this simulation model these losses by a coefficient called" Dissociation coefficient" noted ξ_d and defined by the following relationship: $\xi_d = 1 - \frac{\Delta P_d}{Pci}$ where Pci-is the lower heating value of fuel

$$\Delta P_d = n_{CO}.Q_{CO} + n_{H_2}.Q_{H_2} + n_H.Q_H + n_{OH}.Q_{OH} + n_{NO}.Q_{NO} + n_O.Q_O$$

heat losses due to the dissociation of combustion products. n_i number of moles of species i and Q_i heat of reaction(enthalpy of formation)

3.2.5 The heat losses due to incomplete combustion (case of a rich mixture ϕ<1) are caracterised in our study by a coefficient called «coefficient of incomplete combustion », noted δ and defined by the following relationship: $\delta = 1 - \frac{\Delta P_{ci}}{P_{ci}}$ where: $\Delta P_{ci} = 119950.(1 - \frac{1}{\phi}).L_{ov}$ (kJ kg^{-1} of fuel) are the heat losses due to incomplete combustion

Where $L_{ov} = \frac{1}{0.208}.\left[\frac{C}{12} + \frac{H}{4} - \frac{O}{32}\right]$, (kmol of air kg^{-1} fuel) is the number of moles of air required for stoichiometric combustion of 1 kg of fuel

C,H,O - is the fuel composition percent by mass of C, H_2 and O_2 .

ϕ - is the fuel/air equivalence ratio.

3.2.6 We propose an initial dissociation coefficient (ξd = 0.9) the same in the ten zones.

3.2.7 The heat actually released during the combustion is calculated from the following relationship: $Q_z = \frac{R_{pc}.P_{ci}}{n_{mc}.\left(1 + \gamma_r\right)}$ where $R_{pc} = \xi_d.\delta$ is the efficiency of combustion, n_{mc} is the number of moles of the carburated mixture and γ_r is the residual fraction.

3.2.8 Compute the mass fraction burned in each zone by the following equation: $\Delta XI = \frac{0.999}{N_z}$ where N_z= 10 is the number of zones.

3.2.9 Compute the combustion duration in each zone $\Delta\varphi_j$ from the Wiebe law by the following equation:

$$\Delta\varphi_j = \varphi_j - \varphi_{j-1} = \varphi_z.\left\{\left[-\frac{\ln(1-X_j)}{6.908}\right]^{\frac{1}{(m+1)}} - \left[-\frac{\ln(1-X_{j-1})}{6.908}\right]^{\frac{1}{(m+1)}}\right\}$$

where $1 \le j \le N_z$-1 and $X_j = X_{j-1}+\Delta XI$ and $\Delta\varphi_{N_z} = \varphi_z$ - is the total combustion duration.

3.2.10 At the start of combustion: $\alpha_1 = \theta$, $\varphi_1 = 0$, $X_1 = 0$, where θ is the ignition timing. Compute V_1 from engine geometry. The first temperature of working-fluid in unburnt zones (all zones) is equal to the mixture temperature at the end of compression $T_{uf} = T_2$.

3.2.11 For new crank angle $\varphi_2 = \varphi_1+\Delta\varphi$, $\alpha_2 = \alpha_1+\Delta\alpha$, where $\Delta\varphi = \Delta\alpha$ equal to 1°. compute V_2 from engine geometry and then calculate the new temperature at the end of step from the following equation $T_2 = T_1+\Delta T$, where ΔT is the proposed increment of temperature in this step.

3.2.12 Compute the mass fraction burned X_2 at the end of step from the Wiebe law:

$$X_2 = 1 - \exp\left[-6.908.\left(\frac{\varphi_2}{\varphi_z}\right)^{(m+1)}\right]$$

where m and φ_2 is the kinetic parameters calculated from measured pressure diagram for each experimental point. Find the mean mass fraction burned X_{1-2} in the step 1-2 by the following equation:

$$X_{1-2} = \frac{(X_1 + X_2)}{2}$$

3.2.13 Calculate the mean molar expansion coefficient of working-fluid β_{1-2} in the step 1-2 by the following equation:

$$\beta_{1-2} = 1 + (\beta_{max} - 1).X_{1-2}$$

where $\beta_{max} = \frac{\beta_{o.max} + \gamma_r}{(1+\gamma_r)}$ and

$$\beta_{o.max} = \begin{cases} 1 + \dfrac{\frac{H}{4} + \frac{O}{32} + 0.21.(1-\frac{1}{\phi}).L_{ov} - \frac{1}{M_f}}{\frac{L_{ov}}{\phi} + \frac{1}{M_f}} & \text{if } \phi \ge 1 \\ 1 + \dfrac{\frac{H}{4} + \frac{O}{32} - \frac{1}{M_f}}{\frac{L_{ov}}{\phi} + \frac{1}{M_f}} & \text{if } \phi < 1 \end{cases}$$

where $\beta_{o.max}$ is the maximum molar expansion coefficient of carbureted mixture;
β_{max} is the maximum molar expansion coefficient of working-fluid;
M_f is the molecular weight of fuel
ϕ is the fuel/air equivalence ratio.

3.2.14 Compute the mean temperature in this step $T_{1-2} = \frac{(T_1 + T_2)}{2}$, the mean isentropic exponent

$$K_{1-2} = \begin{cases} 1.259 + \left[76.7 - (13.6 - 14.2.\phi).X_{1-2}\right].\dfrac{1}{T_{1-2}} \\ -(0.0665 - 0.0245.\phi).X_{1-2} \quad \text{if } \phi \ge 1 \\ 1.259 + \left[76.7 + 0.6.X_{1-2}\right].\dfrac{1}{T_{1-2}} - (0.012 + 0.03.\phi) \\ .X_{1-2} \quad \text{if } \phi < 1 \end{cases}$$

and the mean molar heat capacity

$$C_v(T_{1-2}) = \frac{R}{M_{mix}.(K_{1-2} - 1)}$$

3.2.15 Find pressure P_2 at the end of step from the first law of thermodynamics for a closed system:

$dU = \delta Q_h + \delta Q_X + \delta W$ where $\delta Q_X = R_{pc}.P_{ci}.g_c.dX$

where g_c - is the admitted mass per cycle.
dX-The mass fraction burned calculated from Wiebe law[17].

3.2.16 Estimate temperature at the end of step

$$T_{2e} = T_1.\frac{P_2}{P_1}.\frac{V_2}{V_1}.\frac{1}{\beta_{1-2}}$$

3.2.17 Repeat steps 3.2.14 to 3.2.16 until the error (T_{2e}-T_2) is negligible.

3.2.18 Calculate the work in the step:

$$\delta W = \frac{(P_1 + P_2)(V_2 - V_1)}{2}$$

3.2.19 Estimate the temperature of working fluids in unburnt zones at the end of step by the following equation: $T_{u2} = T_{uf} + \Delta T_u$,where ΔT_u is the proposed increment of temperature of working fluids in unburnt zones in this step.

3.2.20 Compute the mean temperature of working-fluid in unburnt zones in this step $T_{um} = \frac{(T_{u2} + T_{uf})}{2}$, calculate the mean heat capacity of the working-fluid $C_v(T_{um})$ and $C_p(T_{um})$ by the following equations:

$$C_{v.wmix}(T_{um}) = \frac{\left[C_{v.cmix}(T_{um}) + \gamma_r . C_{v.egr}(T_{um})\right]}{\left(1+\gamma_r\right)},$$

$$C_{p.wmix}(T_{um}) = C_{v.wmix}(T_{um}) + R$$

where: $C_{v.cmix}(T_{um}) = C_{v.air}(T_{um}) = a_{air} + b_{air}.T_{um}$ is the mean heat capacity of carbureted mixture (assumed to be that of air);

$$C_{v.egr}(T_{um}) = \sum_{i=1}^{5} \upsilon_i . C_{v.i}(T_{um}) = \upsilon_{CO2}.C_{v.CO2}(T_{um}) + \upsilon_{H2O}.C_{v.H2O}(T_{um}) + \upsilon_{CO}.C_{v.CO}(T_{um}) + \upsilon_{H2}.C_{v.H2}(T_{um}) + \upsilon_{N2}.C_{v.N2}(T_{um})$$

is the mean heat capacity of residual gases; v_i is the molar fraction of species i $C_{v.i}(T_{um}) = a_i + b_i.T_{um} + c_i.T_{um}^2$ is the mean heat capacity of species i.

3.2.21 Calculate the mean isentropic exponent $\gamma_{u.wmix}$ of the working-fluid in the unburnt zones by the following equation:

$$\gamma_{u.wmix}(T_{um}) = \frac{C_{p.wmix}(T_{um})}{C_{v.wmix}(T_{um})}$$

3.2.22 Find the temperature of working fluids in unburnt zones at the end of this step T_{u2} assuming isentropic change:

$$T_{u2'} = T_{uf}.\left(\frac{P_2}{P_1}\right)^{\frac{\left(1-\gamma_{u.wmix}(T_{um})\right)}{\gamma_{u.wmix}(T_{um})}}$$

3.2.23 Repeat steps 3.2.20 to 3.2.22 until the error ($T_{u2'}$-T_{u2}) is negligible. In order to accelerate the convergence of the numerical procedure, the increase in temperature Δt_u for the next step is calculated by an extrapolation method ($\Delta T_u = T_{u2'} - T_{uf}$).

3.2.24 Set conditions at the end of time step (index 2) as initial conditions for the next time step (new state, index 1) and repeat all steps from 3.2.10 to 3.2.23. Carry on this way, until φ_2 equals the value of combustion duration of the zone j (j is the number of zone), i.e., $\varphi_2 = \Delta\varphi_j$ were $1 \le j \le N_z = 10$

3.2.25 We suppose that the combustion products appear ssuddenly(instantaneously) when the flame front riches the end of this zone(i.e., $\varphi_2 = \Delta\varphi_j$). At this instant we apply the first law of thermodynamics between the beginning and the end of combustion of the considered zone(we designate it by w, i.e., j = w):

$$\Delta Q_w = \left(U''_{p.c}\right)_w - \left(U'_{w.mix}\right) + \sum_{k=1}^{w-1}\left(\Delta U_{p.c}\right)_k + \sum_{k=w+1}^{N_z=10}\left(\Delta U_{w.mix}\right)_k + \Delta W_w$$

where: $\Delta Q_w = \xi_{dwi}.(P_{ci} - \Delta P_{ci}).\Delta X_w$ is the heat actually released by combustion in zone w, initially we set: $\xi_{dwi} = \xi_d$

$$\left(U''_{pc}\right)_w = \sum_{i=1}^{11} n_i . C_{v.i}\left(\left(t''_{pc}\right)_w\right).\left(t''_{pc}\right)_w .\Delta X_w$$

$$= \sum_{i=1}^{11} n_i .\left[a_i + b_i .\left(t''_{pc}\right)_w\right].\left(t''_{pc}\right)_w .\Delta X_w$$

is the final internal energy of the combustion products (11 species) in zone w.

We put:

$$A = \sum_{i=1}^{11} n_i .a_i = n_{CO2}.a_{CO2} + n_{CO}.a_{CO} + n_{H2O}.a_{H2O} + n_{H2}.a_{H2} + n_{OH}.a_{OH} + n_{O2}.a_{O2} + n_O.a_O + n_{NO}.a_{NO} + n_{N2}.a_{N2} + n_H.a_H + n_N.a_N$$

$$B = \sum_{i=1}^{11} n_i .b_i = n_{CO2}.b_{CO2} + n_{CO}.b_{CO} + n_{H2O}.b_{H2O} + n_{H2}.b_{H2} + n_{OH}.b_{OH} + n_{O2}.b_{O2} + n_O.b_O + n_{NO}.b_{NO} + n_{N2}.b_{N2} + n_H.b_H + n_N.b_N$$

Therefore the first law can be written in these conditions as follows :

$$B.\left(t''_{pc}\right)_w^2 + A.\left(t''_{pc}\right)_w - C = 0$$

Where

$$C = \frac{1}{\Delta X_w}.\left\{\begin{array}{l}\Delta Q_w + \left(U'_{w.mix}\right) - \sum_{k=1}^{w-1}\left(\Delta U_{p.c}\right)_k \\ - \sum_{k=w+1}^{N_z=10}\left(\Delta U_{w.mix}\right)_k - \Delta W_w\end{array}\right\}$$

The temperature of the combustion products in zone w at the time when the flame front reaches the end of this zone is therefore the positive root of the above second order equation:

$$\left(t''_{pc}\right)_w = \frac{-A + \sqrt{A^2 + 4.B.C}}{2.B};°C \text{ and } \left(T''_{pc}\right)_w = \left(t''_{pc}\right)_w + 273;K$$

3.2.26 Knowing the temperature of the combustion products in zone w $(T''_{pc})_w$, the pressure P_2, the equivalance ratio ϕ and the rate of residual gases γ_r we calculate again the number of moles of the 11 species in the combustion products, their molar fractions and also the new local dissociation coefficient in zone w (noted ξ_{dwn}). This calculation is achieved using a subprogram which computes equilibrium combustion products using the element balance equations (one equation for each element C-H-O-N) and equilibrium constants for seven nonredundant reactions, which provides a set of 11 equations required for solution of these species concentrations.

3.2.27 Repeat steps 3.2.25 to 3.2.26 until the error $(\xi_{dwn}-\xi_{dwi})$ is negligible.

3.2.28 Compute the quantity of NO in the burning zone through the chemical kenetics scheme described in a previous section, by solving the relevant differential equation for NO with a fourth-order Runge-Kutta numerical scheme.

3.2.29 At the end of combustion process, i .e., $(\varphi_2 = \varphi_z)$, compute the global dissociation coefficient $(\xi_d)_g$ with the following equation:

$$\left(\xi_d\right)_g = \sum_{i=1}^{N_z=10}\left(\xi_{din}\right).\Delta X_i$$

3.2.30 Repeat steps 3.2.7 to 3.2.29 until the relative error $\frac{\left(\xi_d\right)-\left(\xi_d\right)_g}{\left(\xi_d\right)}$ becomes less than a specified accuracy criterion.

Computation of expansion phase:

3.3.1 At the end of combustion $(\varphi_2 = \varphi_z)$, we have: $\beta_{1-2} = \beta_{max}$, $X_{1-2} = 0.999$ and $dQ_x = 0$ and we use the same algorithm as that of combustion.

3.3.2 Repeat the above steps until the end of the closed cycle (at the EVO event).

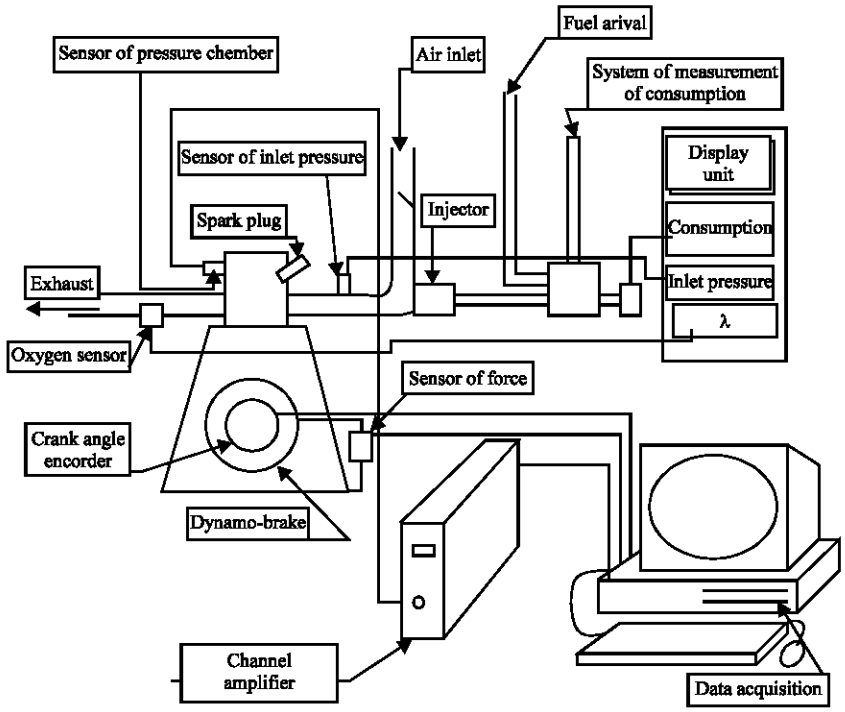

Fig 2: Experimental apparatus

Experimental procedure: Measurements were performed with the apparatus shown in Fig. 2. The brake is an electrical machine mounted in balance and to which the engine is coupled. It can function as a brake (receptor) or as an electric engine according to whether the heat engine delivers energy or is entrained. The role of this unit is to be able to entrain the heat engine at constant speed no matter how much the quantity of energy absorbed or released by it. The control units allow to adjust the rotational speed of the set engine-dynamo (by acting on the dynamo), the mass of air admitted by cycle (by acting on the dynamo), the mass of fuel injected by cycle (by acting on the duration of opening of the electromagnetic injector). This action allows the adjustment of the richness measured with the oxygen sensor. Measurements instruments allow the measure of the delivered or the absorbed couple and the rotational speed of the engine, the angular position, the injected mass of fuel, the richness, the mass of air and the rate of recirculation of the exhaust gases (the EGR). The latter is evaluated via a measure of CO_2 content.

Various experimental results were obtained on the experimental bench of monocylinder spark ignition engine 4JS of the Orleans LME laboratory, using petrol 95 as a fuel. The results are presented in the form of graphs or tables. The values of the pressure in the combustion chamber, of the angular position of the crankshaft during 100 engine cycles, of the average couple and the rotational speed are acquired using a PC. Using these quantities, the PC computes the following quantities:

PME, mean value of the effective mean pressure

PMIBP, mean value of the indicated mean pressure of the cycle low pressure loop, representative of the engine work used to push the fluid in and out of the chamber.

PMIHP, mean value of the indicated average pressure of the cycle high pressure loop representative of the useful work of the pressure on the piston.

PMI, mean value of the indicated average pressure, sum of the preceding two.

PMF, mean value of friction pressure, representative of the losses by mechanical friction in the engine.

P_{max}, Maximum pressure attained during a cycle

α_{Pmax}, angle for which the maximum pressure is attained

σ_{PMI}, typical deviation of the indicated mean pressure

σ_{PMI}/PMI, variation coefficient, which may be considered as a characteristic of the stability of the functionning of the engine.

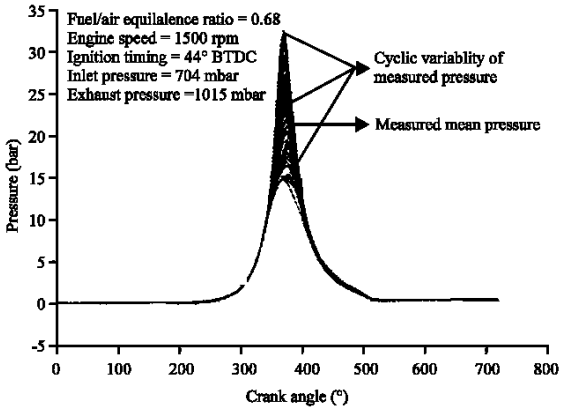

Fig. 3: Variationof the mean pressure in the cylinder as a function of crankshaft angle for 100 consecutive cycles related to experiment: r0.68n1500

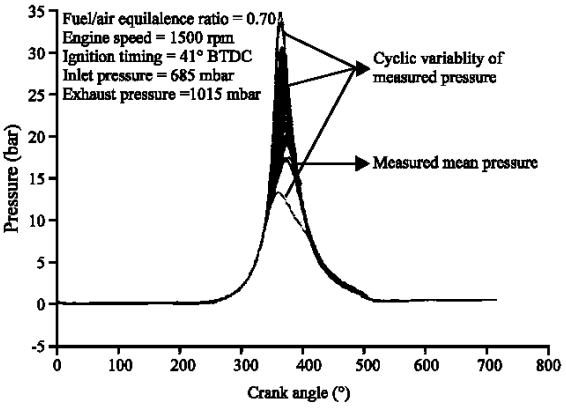

Fig. 4: Variation of the mean pressure in the cylinder as a function of crankshaft angle for 100 consecutive cycles related to experiment: r0.70n1500

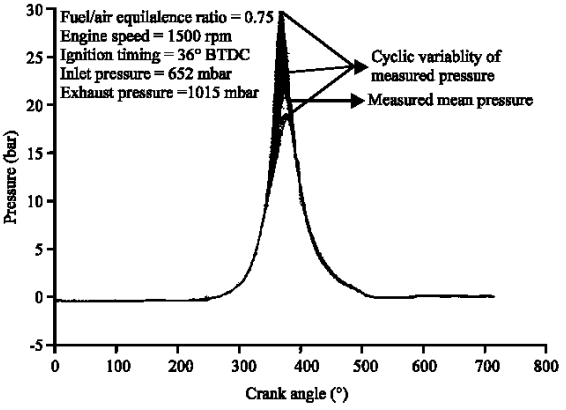

Fig. 5: Variation of the mean pressure in the cylinder as a function of crankshaft angle for 100 consecutive cycles related to experiment: r0.75n1500

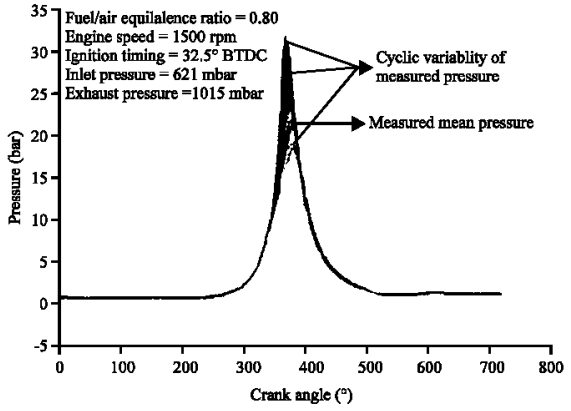

Fig. 6: Variation of the mean pressure in the cylinder as a function of crankshaft angle for 100 consecutive cycles related to experiment: r0.8n1500

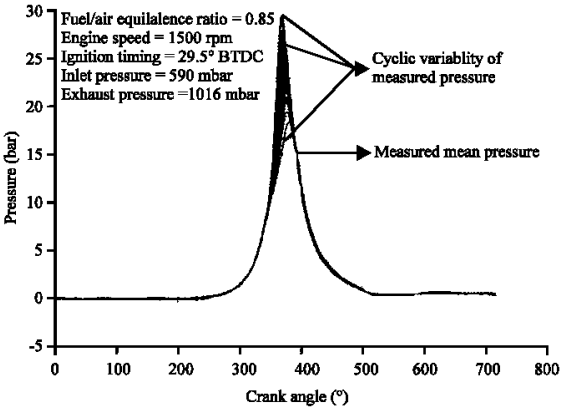

Fig. 7: Variation of the mean pressure in the cylinder as a function of crankshaft angle for 100 consecutive cycles related to experiment: r0.85n1500

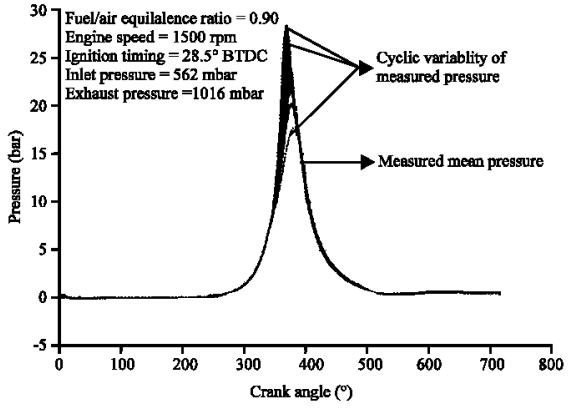

Fig. 8: Variation of the mean pressure in the cylinder as a function of crankshaft angle for 100 consecutive cycles related to experiment: r0.9n1500

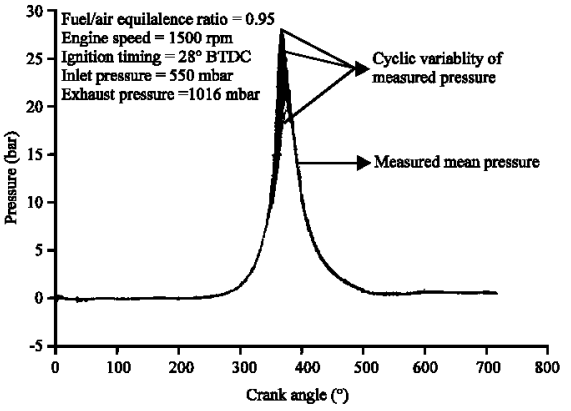

Fig. 9: Variation of the mean pressure in the cylinder as a function of crankshaft angle for 100 consecutive cycles related to experiment: r.95n1500

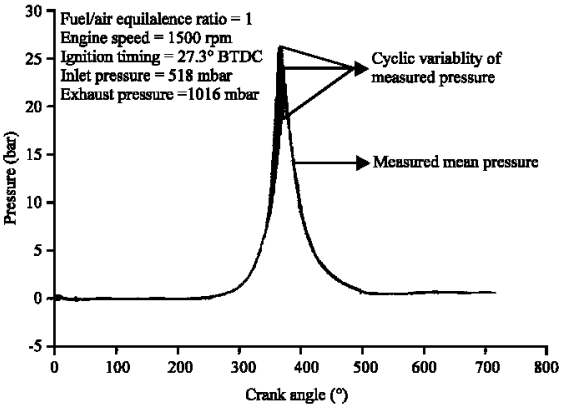

Fig. 10: Variation of the mean pressure in the cylinder as a function of crankshaft angle for 100 consecutive cycles related to experiment: r1n1500

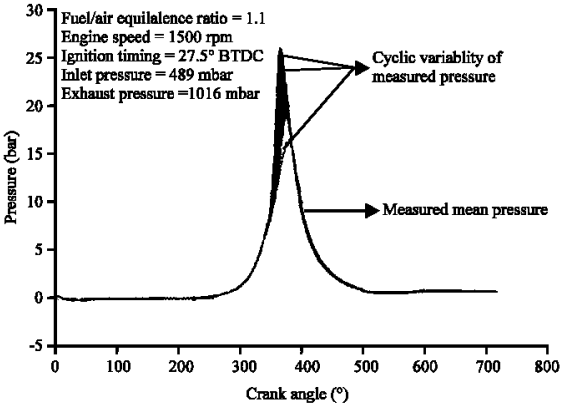

Fig. 11: Variation of the mean pressure in the cylinder as a function of crankshaft angle for 100 consecutive cycles related to experiment: r1.1n1500

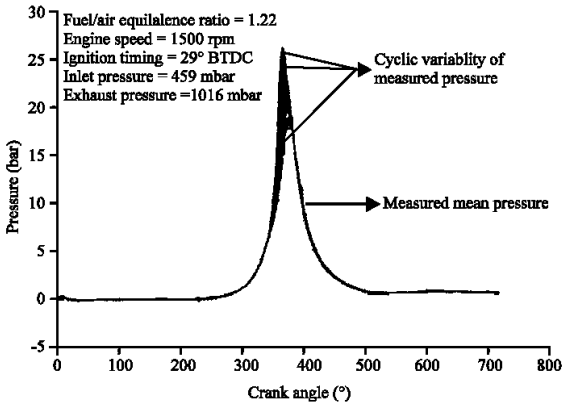

Fig. 12: Variation of the mean pressure in the cylinder as a function of crankshaft angle for 100 consecutive cycles related to experiment: r1.22n1500

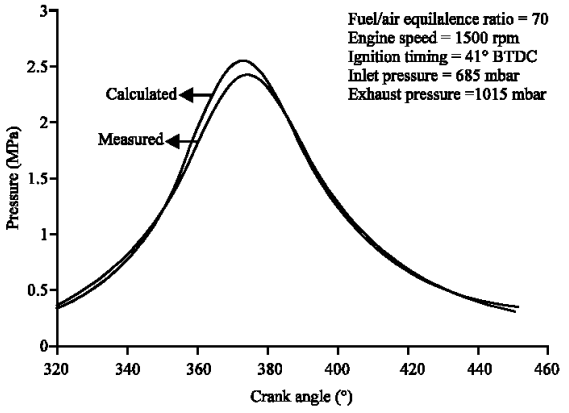

Fig. 13: Comparison between the mean measured and predicted mean pressure related to experiment r.70n1500

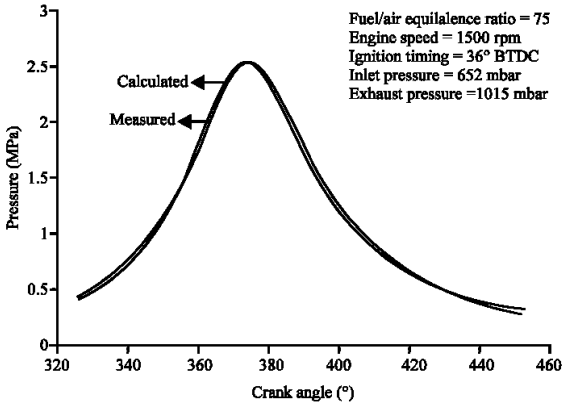

Fig. 14: Comparison between the measured and predicted pressure related to experiment r0.75n1500

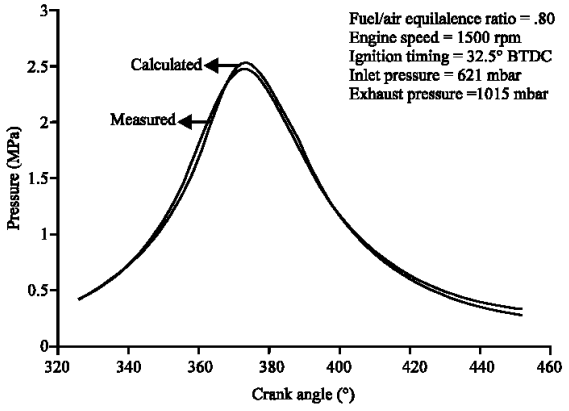

Fig. 15: Comparison between the measured and predicted mean pressure related to experiment r0.8n1500

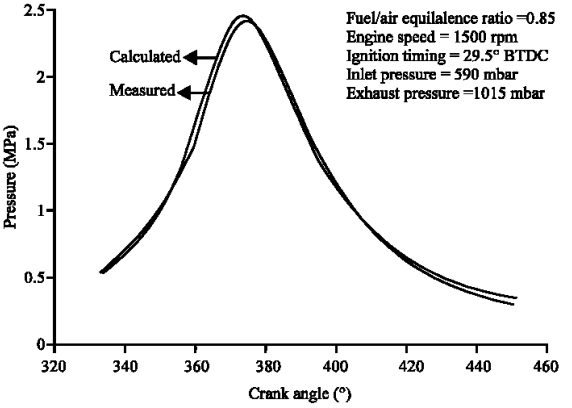

Fig. 16: Comparison between the measured and predicted mean pressure related to experiment r0.85n1500

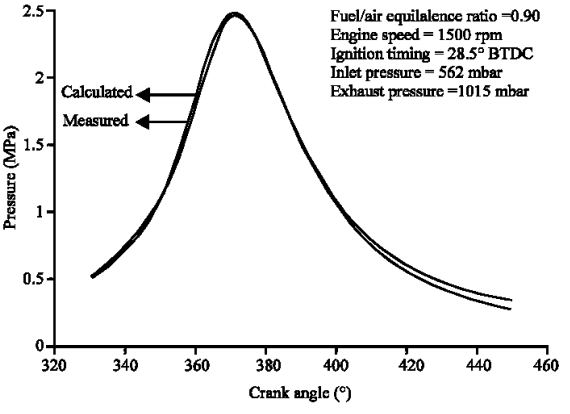

Fig. 17: Comparison between the measured and predicted mean pressure related to experiment r0.9n1500

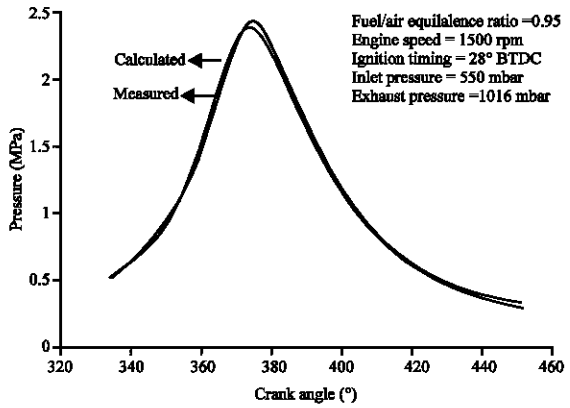

Fig. 18: Comparison between the measured and predicted mean pressure related to experiment r0.95n1500

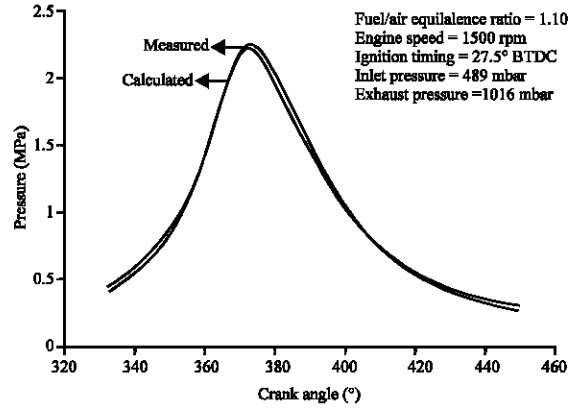

Fig. 19: Comparison between the measured and predicted mean pressure related to experiment r1.1n1500

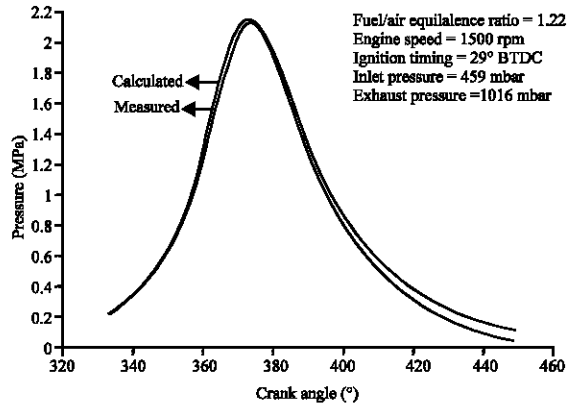

Fig. 20: Comparison between the measured and predicted mean pressure related to experiment r1.22n1500

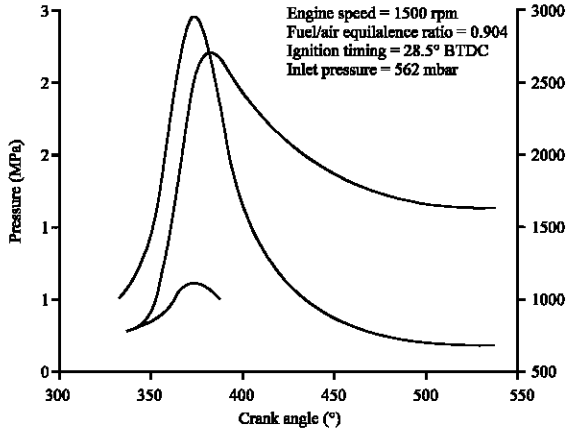

Fig. 21: Variation of the cylinder pressure(P), of the mean temperature of fresh gases (Tgf) and that of the combustion products(Tpc) as a function of crankshaft angle

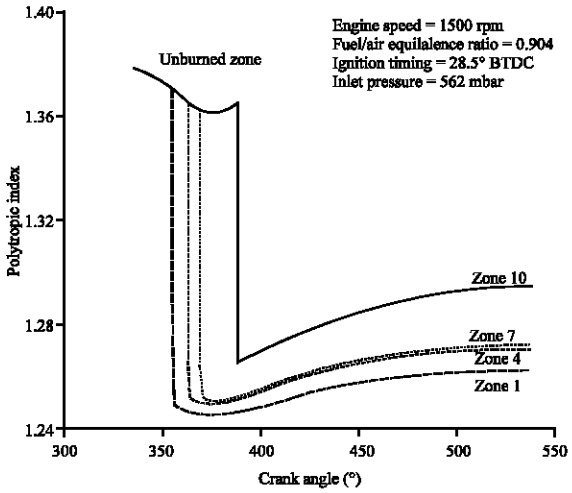

Fig. 22: Evolution of the mean polytropic exponent Of fresh gases (γ_{GF}) and that of the combustion products (γ_{PC1}, γ_{PC4}, γ_{PC7}, γ_{PC10}) as a function of crankshaft angle

For a rotational speed of 1500 revolutions/mn and a constant mass flow rate of the fuel (10.77g mn^{-1}), We studied the influence of the richness of the carburated mixture (We have realised 10 measurement points) on the functionning charateristics of the engine and on the formation of pollutants and in particular the NOx.

For a better representativity of the experimental results and due to the cyclic dispersion observed during the pressures acquisition, We have presented graphs of the variation of the cylinder pressure as a function of the crankshaft angle for the mean cycle Fig. 3-12. The measured variations of temperature of fresh gases,

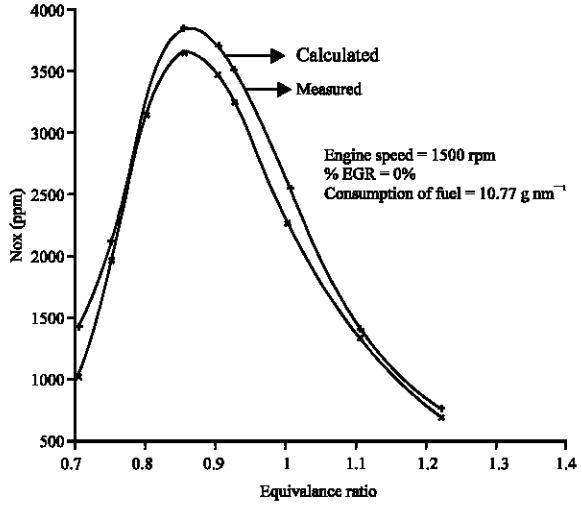

Fig. 23: Comparison between the measured and predicted concentration of NOx as a function of the richness

combustion products and pressure over a cycle are shown in Fig. 21. A comparison between the experimental data and the computed values is presented in this study for the mean gas pressure (Fig. 13-20) and for the NOx emissions (Fig. 23)

RESULTS AND DISCUSSION

The experiments were realised on the experimental bench belonging to the Mechanics and Energetics Laboratory (LME) of the Polytechnic school of the University of Orleans(France). The engine for which the data was obtained is a monocylinder which possesses the following essential geometrical characteristics Table 2.

Figures 3 to 12 give the measured mean pressure in the cylinder as a function of the richness of the carburated mixture and the ensuing operating parameters(ignition timing, inlet and exhaust pressures) for a rotational speed of 1500 rpm and for 100 consecutive cycles. The results show a very good repeatability of the data over the 100 cycles and a clear decrease in the maximum pressure as the richness of the mixture increases.

Before the validation of our multizone model in terms of NOx emissions, we first proceed to a comparison of the measured mean pressure(average of 100 consecutive cycles) with the computed pressure using the 0D model. Figures 13-20 illustrate the comparison between the mean cycle of the measured pressure and that predicted by our 0D model for richnesses varying from $\phi = 0.7 \div 1.22$. For each experimental point, We first determine the kinetic parameters figuring in Wiebe's law, i.e.,: the exponent of

Table 2: Characteristics of the monocylinder engine

Number of cylinders	1
Compression ratio	10.1
Number of inlet valves	2
Number of exhaust valves	2
Diameter of inlet valves	Di = 29.5 mm
Diameter of exhaust valves	De = 26.6 mm
Bore	Al = 88 mm
Stroke	A2 = 82 mm
Crank radius	R = 41 mm
Connecting road length	L = 138 mm
Angle of inlet valve	Beta = 16.25°
Angle of exhaust valve	Gamma = 15.67°

Table 3: Comparaison between the measured and predicted concentration of NOx for various values of the richness of the carburated mixture

fuel/air equivalence ratio ϕ	0.70	0.75	0.80	0.85	0.90	0.95	1.00	1.11	1.22
NOx (ppm) measured	1029	1964	3143	3638	3475	3236	2255	1341	705
NOx (ppm) calculated	1435	2140	3260	3842	3698	3512	2562	1412	775

the character of combustion (noted m), the angular duration of combustion process (noted ϕ_z) and also the quantity of heat generated during the combustion process to 1 m^3 of gases (noted q_{zp}). These parameters are then introduced in the principal programme. From these figures one can notice a very acceptable and very encouraging accord between the measured pressure and that predicted by our model for different richnesses of the carburated mixture entering the cylinder.

Figure 21 shows clearly the relationship between the temperature and pressure during a cycle. The maxima of these parameters occur at the same crankshaft angle, corresponding to complete combustion. This figure also shows the increase in the fresh products temperature as they are compressed before ignition.

Figure 22 shows the value of the polytropic exponent as a function of the crankshaft angle. The values before combustion (fresh mixture) are near to those of air, whereas the lowest values can be observed for the first zones, where temperatures are highest.

The trends in temperature variations are reflected in the concentration of NOx . Figure 23 shows a comparison of the measured NOx emissions with those predicted by the developed multizone model. As one can clearly notice on this Figure and on Table 3, with the increase in the richness ($0.7 \leq \phi < 0.85$) the concentration of NOx increases first(this increase being essentially due to the increase of the maximum temperature of the cycle). The reason being that with the increase of richness in the interval considered (from 0.7 to 0.85), the effect of temperature increase of the gases counterbalances the decrease of the O_2 partial pressure and the peak of emission curve for NO (about 3638 p.p.m) appears for a

Table 4: Predicted values of the local and global dissociation coefficients in the zônes for various values of the richness of the carburated mixture

fuel/air equivalence ratio	Local(KD_i)and global(KD_G) dissociation coefficients in the zônes (%)										
	KD_1	KD_2	KD_3	KD_4	KD_5	KD_6	KD_7	KD_8	KD_9	KD_{10}	KD_G
0.70	89.5	98.7	98.7	98.8	98.8	98.9	99	99.2	99.9	99.6	92.8
0.75	91.1	97.5	97.5	97.4	97.4	97.4	97.5	97.7	98.1	99.8	99.8
0.80	91.7	96.9	96.8	96.6	96.6	96.6	96.6	96.8	97.2	99.6	96.6
0.85	90.3	96	95.8	95.8	95.6	95.8	95.7	95.8	96.3	99.6	95.6
0.90	89	95.4	95.3	95.3	95.1	95.3	95.2	95.5	96.1	99.8	95.2
0.95	87.5	94.9	94.8	94.9	94.8	94.8	94.8	95	95.6	99.7	94.7
1.00	85.4	93.2	93.3	93.1	93.4	93.1	93.4	93.6	94.5	99.8	93.4
1.11	91	97.3	97.3	97.4	97.3	97.3	97.4	97.5	97.9	99.8	97
1.22	96	99.1	99	99	99	99	99	99	99.3	99.7	98.7

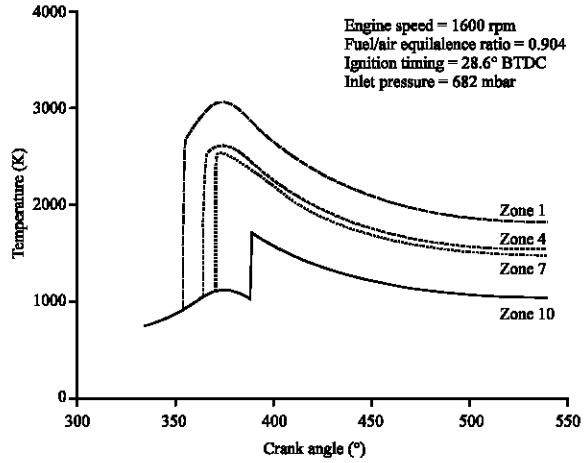

Fig. 24: Evolution of the local temperature (K) in zones 1, 4,7 et 10 as a function of crankshaft angle

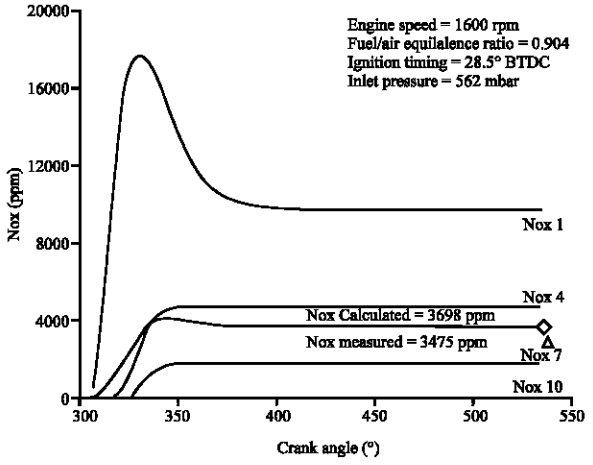

Fig. 25: Variation of the global concentration of NOx (in the 10 zones) et local concentration (ppm) in zones 1, 4,7 et 10 as a function Of crankshaft angle related to experiment r0.9n1500.

richness of about 0.85, the NO concentration then diminishes consequent to the decrease of the maximum combustion temperature.

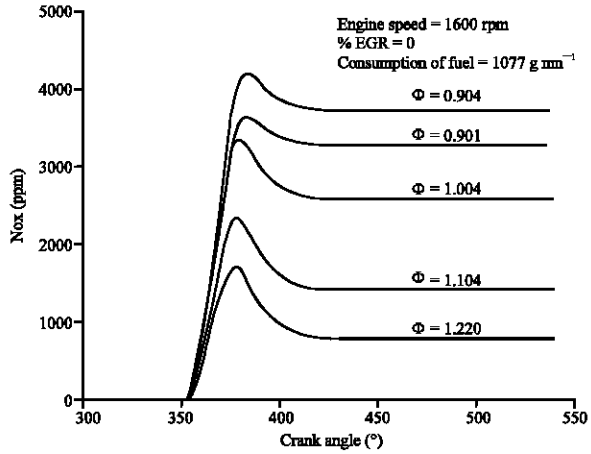

Fig. 26: Variation of the global concentration of NOx (in the 10 zones) as a function of crankshaft angle for various values of the richness of the carburated mixture.

In all the considered cases (no matter the value of the richness is), the zones which burn first exert the biggest contribution to the formation of NOx. The reason being that these zones possess at the same time the highest temperature ($Tpc1 < T_{pc2} < T_{pc3} < T_{pc4} < T_{pc5} < T_{pc6} < T_{pc7} < T_{pc8} < T_{pc9} < T_{pc10}$) Fig. 24 and the biggest period of stay of the combustion products

$$(\varphi_1 = 36^\circ dv, \varphi_2 = 36^\circ dv, \varphi_3 = 36^\circ dv, \varphi_4 = 36^\circ dv, \varphi_5 = 36^\circ dv, \varphi_6 = 36^\circ dv, \varphi_7 = 36^\circ dv, \varphi_8 = 36^\circ dv, \varphi_9 = 36^\circ dv, \varphi_{10} = 36^\circ dv),$$

which favors the most important formation of nitrogen oxides in these zones ($NOx1 > NOx_2 > NOx_3 > NOx_4 > NOx_5 > NOx_6 > NOx_7 > NOx_8 > NOx_9 > NOx_{10}$) Fig. 25. Moreover, an other very important result is that the level of NOx formation in the first zones is controlled simultaneously by the phenomenons of formation and decomposition, whereas in the other remaining zones this level is controlled only by the phenomenon of formation. This

can be explained by the fact that the heat losses via the dissociation of the combustion products are greater in the first zones than in the remaining zones (Table.4), for example corresponding to a richness $\phi = 0.70$, we have : [KD_1= 89.5% (10.5% of losses by dissociation)], [KD_2= 98.7% (1.3% of losses by dissociation)], [KD_3 = 89.7% (1.3% of losses by dissociation)], [KD_4= 98.8% (1.2% of losses by dissociation)], [KD_5= 98.8% (1.2% of losses by dissociation)], [KD_6= 98.9% (1.1% of losses by dissociation)], [KD_7= 99% (1% of losses by dissociation)], [KD_8= 99.2% (0.8% of losses by dissociation)], [KD_9= 99.9% (0.1% of losses by dissociation)], [KD_{10}= 99.6% (0.4% of losses by dissociation)]. This is the reason why the concentration of NOx diminishes from the first to the last zone.

According to the theory by Zeldovich, the speed of formation of NO is determined by the maximum temperature in the reaction zone and also by the concentration of oxygen and nitrogen. One notices from Fig. 21 and 26 that with a poor carburated mixture, the concentration of NO increases in the beginning (due to an increase of oxygen concentration and the maximum combustion temperature) and then decreases because of the fall of cycle maximum temperature. It should also be underlined that the poorness of the carburated mixture leads on one hand to a reduction in the quantity of fuel introduced into a cylinder during each cycle and on the other hand to an increase of the heat losses due to the dissociation of the combustion products. These two phenomena are responsible for the fall in maximum temperature, which consequently causes a reduction in the concentration of NO.

CONCLUSION

The general conclusion of our work can be summarised as follows :

- The concordance between the measured values and those predicted by our 0D model is sufficiently good;
- The peak of NOx emissions appears for a richness of about 0.85 (i.e., for a mixture which is slightly poor).
- The greatest quantity of NOx emitted in the exhaust gases comes from the zones which burn first. This is why it is necessary to reduce the temperature of these zones in order to reduce the NOx in the exhaust, this can be achieved for example by the process of a stratified charge or that of prechamber torch ignition.
- The l evel of nitrogen oxides formation in the first zones is controlled simultaneously by the pheno-mena of formation and decomposition, whereas in the other remaining zones, this level is controlled uniquely by the phenomenon of formation. This is explained by the fact that the heat losses due to the dissociation of the combustion products are greater in the first zones than in the remaining zones.

REFERENCES

1. Patterson, D.J. and G. van Wylen, 1964. A Digital Computer Simulation for Spark-Ignited Engine Cycles », in SAE Progress in Technology, «Digital Calculations of Engine Cycles».
2. Krieger,R.B. and G.L. Borman, 1966. The Computation of Apparent Heat Release for Internal Combustion Engines, ASME paper 66-WA/DGP-4.
3. Lavoie, G.A., J.B. Heywood and J.C. Keck, 1970. Experimental and Theoretical Study of Nitric Oxide Formation in Internal Combustion Engines, Combustion and Science Technology, pp: 331-339.
4. Plumberg, P. and J.K. Kummer, 1971. Predictions of NO Formation in Spark-Ignited Engines-An Analysis of Methods of Control, Combustion and Science Technology, p: 73.
5. Heywood, J.B., J.M. Higgins and P.A. Watts and R.J. Tabaczynski, 1979. Development and use of a Cycle Simulation to Predict SI engine Efficiency and Nox Emissions, Society of Automotive Enginneers, SAE.
6. Plumberg, P.N., G.A. Lavoie and R.J. Tabaczynski, 1979. Phenomenological Models for Reciprocating Internal Combustion Engines, Progress in Energy and Combustion Science, pp: 123-167.
7. Lavoie, G. and P. Blumberg, 1980. Combustion Science and Technology, pp: 225-258.
8. James, E.H., 1982. Errors in NO Emission Prediction from Spark Ignition Engines, Society of Automotive Engineers, SAE.
9. Miller, R., G. Davis, C. Newman and T. Gardner, 1998. Asuper-Extended Zel'dovich for Nox Modeling and Engine Calibration, Society of Automotive Engineers, SAE.
10. Rublewski, M. and J.B. Heywood, 2001. Modelling NO Formation in Spark Ignition Engines with a Layered Adiabatic Core and Combustion Efficiency Routine, Society of Automotive Engineers, SAE.
11. Stone, C.R., L.P. Wyszynski and R.R. Raine, 2002. Prediction of NO emissions from Stratified Charge Spark-Ignition Engines, Society of Automotive Engineers, SAE paper no. 2002-01-1139.

12. Caton, J.A., 2001. A Multiple-Zone Cycle Simulation for Spark-Ignition Engines: Thermodynamic Details, in large-Bore Engines, Fuel Effects, Homogenous Charge Compression Ignition, Engine Performance and Suimulation. Proceedings of the 2001 Fall Technical Conference, ed. V.W.Wong, the ASME Internal Combustion Engine Division, Americain Society of Mechanical Engineers, pp: 41-58.
13. Caton, J.A., 2002. A cycle Simulation Including the Second Law of Thermodynamic for a Spark-Ignitin Engine : Implications of the use of Multiple-Zones for Combustion, 2002 SAE International Congress and Exposition, Society of Automotive Engineers, in Modeling of SI Engines, SP-1702, Cobo Hall, Detroit, MI, 4-7.
14. Caton, J.A., 2002. Extension of a Thermodynamic Cycle Simulation to Include Computations of Nitric Oxide Emissions for Spark-Ignition Engines, » Report no.ERL-2002-01? Version 1.0, Engine Research Laboratory, Department of Mechanical Engineering, Texas A and M University.
15. Caton, J.A., 2002. Detailed results for Nitric Oxide Emissions as Determined From Multiple-Zone cycle Simulation for a Spark-Ignition Engine, In Design, Application, Performance and Emissions of Modern Internal Combustion Engine System and Components, Proceedings of the 2002 Fall Technical Conference, ed. V.W.Wong, the ASME Internal Combustion Engine Division, Americain Society of Mechanical Engineers, pp: 131-148.
16. Woschni, G., 1967. A universally applicable equation for the instantaneous heat transfer coefficient in the internal combustion engine. SAE.
17. Takagaki, S.S. and R.R. Raine, 1997. The effects of compression ratio on nitric oxide and hydrocarbon emission from a spark-ignition natural gas fuelled engine, SAE paper 970506 and SP-1248. Also SAE Transactions-J. of Engines.